

Lips Are Lying: Spotting the Temporal Inconsistency between Audio and Visual in Lip-Syncing DeepFakes

Weifeng Liu^{1†}, Tianyi She^{1†}, Jiawei Liu¹, Run Wang^{1*}, Dongyu Yao¹, Ziyou Liang¹

¹ Key Laboratory of Aerospace Information Security and Trusted Computing, Ministry of Education, School of Cyber Science and Engineeringm Wuhan University, China
{weifengliu, tianyishe, jiaweiliu, dongyu.yao, ziyouliang}@whu.edu.cn



Figure 1: A visualization comparison between common deepfakes involves facial attribute editing and our studied lip-syncing deepfakes (LipSync). The former exhibits a substantial forgery area and identity manipulation, such as face swapping, whereas the latter, lip-syncing deepfakes, relies on the synchronization of the minor lip region and given audio, without any alterations to the subject’s identity. As illustrated in the comparison above, discerning the authenticity of an image sequence becomes arduous in the absence of accompanying labels.

Abstract

In recent years, DeepFake technology has achieved unprecedented success in high-quality video synthesis, whereas these methods also pose potential and severe security threats to humanity. DeepFake can be bifurcated into entertainment applications like face swapping and illicit uses such as lip-syncing fraud. However, lip-forgery videos, which neither change identity nor have discernible visual artifacts, present a formidable challenge to existing DeepFake detection methods. Our preliminary experiments have shown that the effectiveness of the existing methods often drastically decreases or even fails when tackling lip-syncing videos.

In this paper, for the first time, we propose a novel approach dedicated to lip-forgery identification that exploits the inconsistency between lip movements and audio signals. We also mimic human natural cognition by capturing subtle biological links between lips and head regions to boost accuracy. To

better illustrate the effectiveness and advances of our proposed method, we curate a high-quality Lip-Sync dataset by employing the SOTA lip generator. We hope this high-quality and diverse dataset could be well served the further research on this challenging and interesting field. Experimental results show that our approach gives an average accuracy of more than **95.3%** in spotting lip-syncing videos, significantly outperforming the baselines. Extensive experiments demonstrate the capability to tackle deepfakes and the robustness in surviving diverse input transformations. Our method achieves an accuracy of up to **90.2%** in real-world scenarios (*e.g.*, WeChat video call) and shows its powerful capabilities in real scenario deployment. To facilitate the progress of this research community, we release all resources at <https://github.com/AaronComo/LipFD>.

1 Introduction

DeepFake refers to an AI-based technology for synthesizing fake media data Dolhansky *et al.* [2020]. The recent advancements in generative models, particularly the emergence

[†]Equal contribution.

*Corresponding author. E-mail: wangrun@whu.edu.cn

of several GAN architectures Karras *et al.* [2019]; Liu *et al.* [2019]; Choi *et al.* [2018] and the diffusion probabilistic models Ho *et al.* [2020], have enhanced the realism and quality of forged videos that can easily deceive humans. The prevalence of DeepFake poses potential security risks, *e.g.*, political elections and identity verification, sparking public concerns.

DeepFake can be bifurcated into entertainment applications and illicit uses Juefei-Xu *et al.* [2022]. As illustrated in fig. 1, the popular DeepFake aims to bring fun to users by swapping face identity information to synthesize new content, such as gender swapping and age regression. Unfortunately, the severe DeepFake is utilized for illicit crimes, including manipulating political propaganda and fabricating pornographic content. The case is particularly alarming in LipSync fraud, where the audio drives the mouth movements on reconstructed video frames. These DeepFakes are generally exploited by malicious actors in real-world scenarios, such as the widely disseminated fabricated videos of Barack Obama saying things he never said on YouTube Suwajanakorn *et al.* [2017], posing significant security threats. The escalating issue of real-time forgery necessitates an effective detector to identify videos generated through LipSync.

Unlike popular DeepFake which manipulates facial attributes or replaces the entire face, LipSync does not tamper with identity and possesses subtle visual artifacts. More seriously, attackers can adaptively erase these visual artifacts through blurring. Since LipSync follows visual modification driven by audio modality, detecting LipSync forgeries naturally involves spotting the inconsistencies between lips and audio. Whereas the correlation between them is closely tied to individual talking styles, intensifying the challenges in developing a universal model to represent this correlation.

Existing studies on DeepFake detection can be classified into unimodal-based and multi-modal-based methods, where the former relies on visual discrepancies arising from identity tampering to detect Lutz and Bassett [2021]; Zhao *et al.* [2020]. However, unimodal detectors become less reliable when the forged videos are perturbed for targeted removal of LipSync artifacts. In recent years, several multi-modal-based methods have emerged Cozzolino *et al.* [2023]; Yang *et al.* [2023]; Hashmi *et al.* [2022], including audio-visual fusion and audio-visual inconsistency. Fusion strategies may confound the learning of singular modality features and the performance post-fusion is not necessarily enhanced Khalid *et al.* [2021]. Muppalla *et al.* [2023] suggested training detectors to learn the inconsistencies between video frames and audio. However, as the arms race between DeepFake creation and detection intensifies, these inconsistencies are gradually reduced, making coarse-grained audio-visual alignment strategies less effective against advanced LipSync methods.

Lip movements are discrete, while the audio spectrum is continuous, resulting in inherent inconsistencies in LipSync videos. As illustrated in the fig. 2, we observe a temporal correlation between the energy variations in audio spectrum and lip movements. To the best of our knowledge, existing works naively align single-frame images with long-range audio clips, thus neglecting the temporal inconsistencies of audio-visual features Agarwal *et al.* [2020]; Mittal *et al.* [2020]. Our experimental evidence also indicates a

marked decline in the efficacy of existing methods when confronting LipSync forged videos. Moreover, Kotsia *et al.* [2008] demonstrated the mouth region’s significance in facial appearance, surpassing even the eyes, due to its biological connections with other head regions. Humans naturally leverage the cues of local regions and head postures to discern facial semantics. While DeepFake technology has made strides in replicating overall facial dynamics, it often falls short of accurately simulating these subtle yet crucial biological interactions. Hence, we choose to exploit the biologically intrinsic correlation between lip movements and head postures as auxiliary information to detect deepfakes. This approach not only mimics the natural cognitive processes of humans but also capitalizes on the existing limitations of deepfakes.

In this paper, for the first time, we propose **LipFD**, a pioneering method that leverages the inconsistencies in audio-visual features for the **Lip-syncing Forgery Detection**. Specifically, our approach captures irregular lip movements that contradict the audio signal aligned with it in the temporal sequence of audio-visual features. We also devise a novel framework that dynamically adjusts the attention of LipFD to regions with different clipping ratios.

To evaluate the effectiveness and generalization of our approach in detecting lip-syncing deepfakes, we utilize the state-of-the-art LipSync methods to generate massive high-quality lip forgery video dataset based on Lip Reading Sentences 2 (LRS2) Afouras *et al.* [2018], Face Forensics++ (FF++) Rossler *et al.* [2019], Deepfake Detection Challenge Dataset (DFDC) Dolhansky *et al.* [2020]. Experimental results show that our approach outperforms prior works by a notable margin, with an accuracy up to **96.93%** for four types of lip forgery videos. Rigorous ablations of our design choices and comparisons with other detection methods demonstrate the superiority of our approach. To summarize, our main contributions are summarized as follows:

- We propose the first-of-its-kind approach dedicated to lip-syncing forgery detection that is often overlooked by existing studies. This method addresses the significant and growing threat of lip-syncing frauds, like those encountered in WeChat video calls.
- In this work, we unveil a key insight that exploits the discrepancies between lip movements and audio signals for fine-grained forgery detection. Our approach introduces a dual-headed detection architecture to enhance detection capabilities.
- We construct the first large scale audio-visual LipSync dataset with nearly one hundred thousand samples, and conducted comprehensive experiments on it alongside other DeepFake datasets. Our method demonstrated high efficacy and robustness, achieving around **94%** average accuracy in LipSync detection, and up to **90.18%** in real-world scenarios.

2 Related Work

Lip-syncing Generation. Lip-syncing facial manipulation, which forges a speaker’s lip movements to match a given audio, is among the most threatening DeepFake applications

due to its subtlety and difficulty to detect, typically falsifying the speaker’s conveyed information. Zhou *et al.* [2020] disentangled the content and speaker information in the audio signal, allowing attackers to generate a forged video using just a single image and an audio segment. Still, it is weak in representing bilabial and fricative sounds due to the omission of short phoneme representations. Prajwal *et al.* [2020] introduced a well-trained discriminator and a temporal consistency checker to address the loss of short-duration phoneme, enhancing the authenticity of generated videos. However, it exhibits weak temporal coordination in the lip movement of talking heads. Wang *et al.* [2023] further focuses on the content of lip movements, making the forgeries challenging for both human eyes and machines to recognize.

DeepFake Detection. The existing DeepFake detectors employ single-modal-based or multi-modal-based approaches to detect subtle differences between real and fake samples. Earlier single-modal detectors aspired to employ neural networks to automatically extract discriminative information Wodajo and Atnafu [2021]; Zhao *et al.* [2021], but they failed to detect unseen samples due to overfitting. To address this issue, some studies shift focus to frequency domain features Liu *et al.* [2021] or subtle forgery artifacts in more generalized datasets Chen *et al.* [2021]; Shiohara and Yamasaki [2022]. Another line is to guide the network to focus on discriminative locations, such as automatically guiding the detector’s positional attention through a double-stream network Shuai *et al.* [2023], or manually cropping the lip region to extract artifacts formed by the inconsistent lip movements Haliassos *et al.* [2021]. Although these works have achieved considerable performance on afore datasets, they are not sensitive when faced with advanced lip-syncing generators due to the absence of synchronized audio features. In the multi-modal-based detectors, noticing that the coordination of audio-visual modalities is an inherently challenging issue in any SOTA generator, Chugh *et al.* [2020] quantifies the disparity between audio and visual as the criterion for classification, but focusing too much on the background information in the video led to failure. In this context, Haliassos *et al.* [2022] intentionally extracts talking head movements and establishes a correlation with audio for discrimination. These methods performed well in addressing audio-visual forgery, but are susceptible to the influence of noise or compression.

3 LipSync Forgery Dataset

To the best of our knowledge, the majority of public DeepFake datasets consist solely of video or image sources, with no specialized dataset specifically dedicated to lip forgery detection available. To fill this gap, we construct a high-quality audio-visual dataset, AVLips, which contains 100,000 audio-visual samples generated by several state-of-the-art LipSync methods. The workflow is demonstrated in fig. 4.

High quality. We employed a combination of static “MakeItTalk” Zhou *et al.* [2020] and dynamic “Wav2Lip” Prajwal *et al.* [2020], “TalkLip” Wang *et al.* [2023] generation methods to simulate realistic lip movements. These generation methods are widely recognized as high-quality work in the academic community, capable of generating high-resolution videos while ensuring accurate lip movements. We

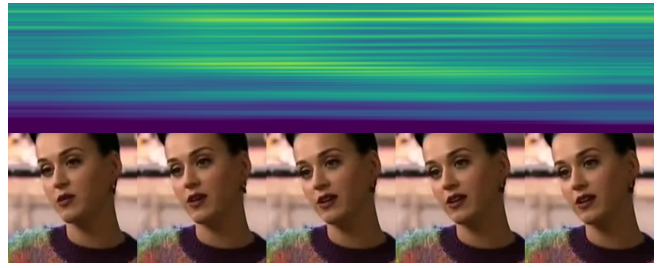


Figure 2: **Real relation between lip movements and spectrogram.** When the woman starts talking, the middle and high frequencies in the spectrum are lighted. As time passes, the energy gradually fades and shifts from the middle frequencies to lower frequencies.



Figure 3: **Lip-syncing fake videos.** The first two frames show a highlighted high-frequency spectrum, which is contradictory to the man not speaking. In the third frame, an unexpected opening of lip appears at the darkest part in the spectrum. On one hand, the mouth cannot change so drastically within a single frame. On the other hand, this lip’s shape contradicts the spectrum information.

applied a noise reduction algorithm to all audio samples before synthesis to reduce irrelevant background noise, ensuring the models can focus on speech content.

Diversity. Our dataset encompasses a wide range of scenarios, covering not only well-known public datasets but also real-world WeChat video calls. Our aim is for this collection to act as a catalyst for advancing real-time forgery detection. To better simulate the nuances of real-world conditions, we have employed six perturbation techniques — saturation, contrast, compression, Gaussian noise, Gaussian blur, and pixelation — at various degrees, thus ensuring the dataset’s realism and practical relevance.

4 Method

In reality, the movements of a speaker’s lip and head are closely intertwined with the spoken content, forming a natural and coherent unity. These physical movements naturally align with the timing and context of the speech. However, the LipSync method, which solely relies on audio signals to generate lip movements frame by frame, only focuses on the precise alignment between lip shapes and speech at any given moment. It overlooks the broader temporal context and the overall coherence of lip and head movements during speech. Consequently, the generated audio-visual outputs often exhibit inherent inconsistencies regarding temporal synchronization. These inconsistencies serve as valuable clues and insights for our detection efforts, highlighting the disparity between natural lip movements and artificially generated ones. Fig. 2 and 3 vividly exhibit the temporal features

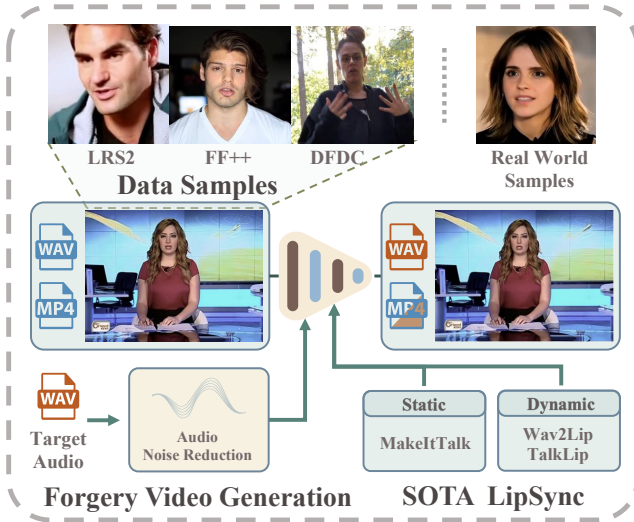


Figure 4: **AVLips dataset construction.** Utilizing static and dynamic methods, we generated high-quality videos with realistic lip movements. The diverse dataset includes various real-world scenarios. Perturbations were applied for robust model training.

among those two classes.

Extracting temporal inconsistencies between audio and video presents notable challenges due to the utilization of features from multiple modalities. To tackle this, we developed a dual-headed detection architecture presented in fig. 5. (1) The Global Feature encoder is dedicated to encoding temporal features, capturing the overarching correlation between audio and lip movements. (2) The Global-Region encoder aims to detect subtle visual forgery traces within regions of varying scales and integrate them with global features. (3) Moreover, we introduced an innovative Region Awareness module that dynamically adjusts the model’s attention across different scales. We will demonstrate in section 6.2 that *this module stands as a cornerstone, harnessing features from regions of diverse sizes, thus empowering our model to effectively capture both the prominent changes in DeepFake and the subtle adjustments in LipSync.*

4.1 Global Feature Encoding

Based on the findings mentioned before, we need to extract features in the temporal domain. Inspired by the translation task in natural language processing, where transformers detect long-distance vocabulary correlations, we regard the inherent correlation between lip movements and spectral information as analogous to the relationship between “vocabulary” in a “sentence” sequence. To capture and encode this correlation, we employ a transformer model.

To effectively carry out its task, the encoder necessitates extraordinary representational capacity, which can be attained through exposure to a vast number of images Ojha *et al.* [2023]. This capacity enables the encoder to accurately allocate attention to the relevant regions of interest. To satisfy this requirement, we choose a variant of vision transformer ViT:L/14 Dosovitskiy *et al.* [2020], pre-trained on CLIP Radford *et al.* [2021]. In our experiments, we use the final layer

of CLIP: ViT-L/14’s visual encoder for image embedding.

Formulation. We denote the convolutional layer as $Conv$, which convolves images down to 224×224 . We first crop source image I into 3 series as $\{c_h^N, c_f^N, c_l^N\}_i$, $i \in \{0, \dots, T-1\}$, where N equals to batch size and T notes the window size. Image I will be embedded into F_G as global feature:

$$F_G = ViT(Conv(I, \theta_{Conv})) \quad (1)$$

$$\{c_h^N, c_f^N, c_l^N\}_i = Crop(I, \{1.0, 0.65, 0.45\}), i \in \{0, 1, 2\} \quad (2)$$

where θ_{Conv} is the parameters of $Conv$. The encoder is constrained by \mathcal{L}_{RA} that is to be further described in the following section.

4.2 Region Awareness

LipSync tends to concentrate on the lower half of the face, and relying solely on coarse-grained global features is insufficient for representation. Therefore, we employ local features to better capture forgery traces.

Formulation. For each crops $c \in \{c_h^N, c_f^N, c_l^N\}_i$, region feature is defined as $F_R = E_{GR}(c, F_G, \theta_{GR})$. We hope this component can focus on the most informative parts of different cropped regions, i.e. lip for c_l and head pose for c_f, c_h . Since lip forgery is often slightly manipulated only on the mouth, the unsupervised model may fail to learn proper representation. We further introduce a region awareness module that applies a modified fully connected layer followed by a sigmoid function, which takes both sub-regions within crops as well as pertinence between region features and their relevant global context into consideration, thus granting different weights to them. The weight is formulated as:

$$\omega_{c_j^i} = RA([F_G | \{F_R\}_j^i], \theta_{RA}), c_j \in \{c_h, c_f, c_l\} \quad (3)$$

where c_j^i denotes the i -th feature in c_j and θ_{RA} is the parameters of region awareness module. The final feature F is:

$$F = \frac{1}{T} \cdot \frac{\sum_{i,j} (\omega_{c_j^i} \cdot [F_G | \{F_R\}_j^i])}{\sum_{i,j} \omega_{c_j^i}} \quad (4)$$

Region Awareness Loss. We noticed that regardless of what high-level patterns the model learned, it is the lips that count. Other information extracted from the spectrogram and head pose should be served as auxiliary. Hence, we designed \mathcal{L}_{RA} , encouraging the region awareness module to focus more on c_l . Mathematically, the loss is defined as:

$$\mathcal{L}_{RA}(\theta_{GR}, \theta_{RA}) = \sum_{j=1}^N \sum_{i=1}^T \frac{k}{\exp(\omega_{max}^i - \omega_h^i)} \quad (5)$$

where ω_{max}^i is the max weight in feature stacks, ω_h^i is the none-cropped region. k is a hyper-parameter used to adjust the steepness of the loss. With \mathcal{L}_{RA} , we expected the model to pay more attention to forged parts.

4.3 Lip Forgery Detection

According to eq. (4), the crop with the highest weight exerts dominance over the feature F , indicating that it encapsulates crucial discriminative information for the final detection.

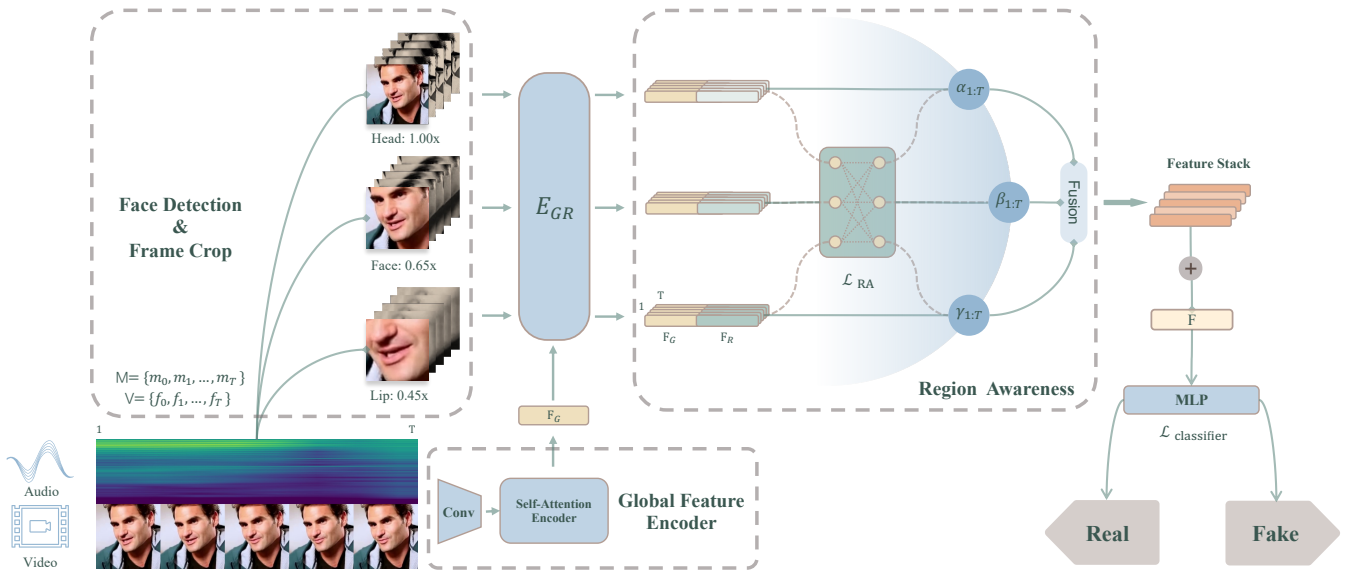


Figure 5: **Overview of LipFD framework.** Blue components represent our main modules in LipFD. The input image was generated by pre-processing, which consists of T frames in the target video and their audio spectrogram. (a) The aim of Global Feature Encoder, a self-attention model, is to extract long-term information between video frames and audio, finding unreasonable correspondences between lip movements and audio. (b) E_{GR} encodes three series of crops, focusing on different parts for each region, and concatenates them with global feature F_G . (c) The Region Awareness module assigns corresponding weights to the features based on their importance. (d) All features are fused together into a unified representation F based on their respective weights for final inference.

Classification. We implement a multi-layer perceptron Taud and Mas [2018] as our classifier optimized with a Binary Cross-Entropy loss:

$$\mathcal{L}_{cls} = -(y \log(F) + (1 - y) \log(1 - F)) \quad (6)$$

where y means the final predicted label. Finally, the objective is given by:

$$\min_{\theta_{RA}, \theta_{cls}, \theta_{GR}} \omega \cdot \mathcal{L}_{RA}(\theta_{GR}, \theta_{RA}) + \mathcal{L}_{cls}(\theta_{cls}) \quad (7)$$

5 Experiment

5.1 Setup

Datasets. We trained our model on Wav2Lip-modified LRS2, a subset of our proposed AVLips. We evaluated our method performance on the following datasets: (1) FF++ Rossler *et al.* [2019], which contains 2,000 samples. (2) DFDC Dolhansky *et al.* [2020], which has 500 samples. (3) AVLips, our proposed dataset, which includes more than 60,000 samples. Since the baselines we compared against were primarily trained on the FF++ or DFDC datasets, to ensure fairness in the evaluation, we regenerated synthetic data for the first two datasets during the testing phase. This approach aims to maintain consistency and provide a level playing field for a fair comparison of the results.

Metrics. Following existing works Chai *et al.* [2020]; Ojha *et al.* [2023]; Dong *et al.* [2022], we adopt four popular metrics to get a comprehensive performance evaluation of LipFD. Specifically, we report ACC (accuracy), AP (average precision), FPR (false positive rate), and FNR (false negative rate). We use the AUC (area under the curve) as a metric to evaluate the performance in tackling various perturbation attacks.

Baselines. We take the SOTA methods in general DeepFake detection and lip-based detection as baselines. (1) For image-based DeepFake detections, UniversalDetect Ojha *et al.* [2023] and SelfBlendedImages Shiohara and Yamasaki [2022] are selected. (2) For video-based DeepFake detections, CViT Wodajo and Atnafu [2021], DoubleStream Shuai *et al.* [2023] and RealForensics Haliassos *et al.* [2022] are considered. (3) For the lip-based detection method, we employ the latest LipForensics Haliassos *et al.* [2021].

5.2 Effectiveness Evaluation

In evaluating the performance of LipFD in detecting Lip-Sync manipulation and the generation across different forgery techniques as well as obtaining a comprehensive performance evaluation, we use four different metrics to report the detection rate and false alarm rate.

Table 1 shows the performance of LipFD and prior works. We take the most advanced general DeepFake detection methods SelfBlendedImages and UniversalFakeDetect, along with representative DoubleStream and CViT video stream detection models as the baseline for DeepFake detection. We also compared our method with the SOTA lip-based method, namely LipForensics, which guides facial judgment through lip pre-reading. In addition, we have also compared the SOTA multi-modal detection method, namely RealForensics.

Experimental results demonstrate that LipFD outperforms all competitors to a significant extent with a high detection rate and low false alarm rate in detecting the three DeepFake datasets. Also, we find that LipFD attains a commendable precision, as evident from the AP metric. Furthermore, we observe some discernible patterns from Table 1.

First, advanced manipulations are hard to detect by general

Method	LRS2 (Ours)				FF++				DFDC			
	ACC \uparrow	AP \uparrow	FPR \downarrow	FNR \downarrow	ACC \uparrow	AP \uparrow	FPR \downarrow	FNR \downarrow	ACC \uparrow	AP \uparrow	FPR \downarrow	FNR \downarrow
CViT [arXiv 2021]	65.54	56.68	0.07	0.61	62.86	54.17	0.24	0.50	70.99	58.06	0.06	0.50
DoubleStream [IWDW 2023]	75.52	67.72	0.13	0.36	<u>91.02</u>	87.64	0.03	0.14	77.39	69.28	0.21	0.24
UniversalFakeDetect [CVPR 2023]	50.03	50.02	0.99	0.01	50.43	50.16	0.99	0.01	49.86	49.94	0.98	0.01
SelfBlendedImages [CVPR 2022]	49.99	52.13	0.07	0.51	64.59	57.93	0.17	0.53	48.47	49.06	0.15	0.50
RealForensics [CVPR 2022]	<u>91.78</u>	<u>90.14</u>	0.02	0.14	50.43	50.16	0.99	0.01	<u>92.54</u>	91.62	0.01	0.14
LipForensics [CVPR 2021]	86.13	81.56	0.18	0.10	51.02	53.48	0.12	0.46	90.75	<u>87.32</u>	0.08	0.11
LipFD (Ours)	95.27	93.08	<u>0.04</u>	<u>0.04</u>	95.10	<u>76.98</u>	<u>0.06</u>	<u>0.05</u>	94.53	78.61	0.08	<u>0.04</u>

Table 1: **Effectiveness in identifying diverse DeepFakes.** Results on LRS2, FF++, and DFDC are reported, including *acc*, *ap*, *fpr*, and *fnr*. The best result is highlighted in bold, while the second-ranking one is underscored. Throughout the entire experiment, the threshold for the AP metric was set to 0.5.

Method	ACC \uparrow	AP \uparrow	FPR \downarrow	FNR \downarrow	AUC \uparrow
Wav2Lip (train, dynamic)	95.27	93.08	0.04	0.04	95.27
MakeItTalk (static)	96.93	95.49	0.02	0.03	96.89
TalkLip (dynamic)	79.33	80.05	0.34	0.04	80.36

Table 2: **Cross-manipulation generalisation.** Evaluation scores when videos are exposed to various unseen forgery algorithms.

methods such as UniversalFakeDetect and SelfBlendedImages, indicating that single-frame-based detectors cannot capture dynamic forgeries. In addition, compared to the SOTA RealForensics method, our ACC exceeded it by 3.8%, 88.5%, and 2.1%, respectively. Similar improvements are reflected in the AP as well. This illustrates that concentrating on lip-syncing allows for the extraction of more potential discriminative features than solely observing lip-based movement.

We observe some bad cases from table 1. For example, the AP score is 13% lower than DoubleStream on the FF++ dataset. On the DFDC dataset, our method has an AP lower than LipForensics and RealForensics by 11% and 16%, respectively. As an explanation, these methods primarily aimed at detecting large-scale manipulations of faces in these types of forgeries. In contrast, LipFD focuses on subtle changes in lip inconsistency. Despite a subtle decrease in balance, LipFD still achieves optimal performance in terms of accuracy.

5.3 Generalizability to Unseen Forgery

A qualified detector is expected to recognize fake videos that were generated using methods *not seen during training*. In this section, we are going to analyze our model’s generalizability by following the protocol used in Chai *et al.* [2020]; Ojha *et al.* [2023]; Dong *et al.* [2022].

Table 2 shows the results of LipFD on various types of methods. Surprisingly, our detector performs even better on data generated by the MakeItTalk method than on the training data itself. This is because MakeItTalk generates dynamic videos by transforming single static images, which inherently lack the coherence of real lip movements. When we use temporal audio-visual information for joint discrimination, it becomes easier to distinguish between real and fake videos.

5.4 Robustness Evaluation

Robustness analysis aims to evaluate the capability of detectors to withstand common perturbation attacks, as corruptive manipulations on videos are prevalent in the wild, especially in the case of forged videos. Following the setup of RealForensics Haliassos *et al.* [2022], we train the model on AVLips without data augmentation and then discuss the robustness of the detectors by testing with unseen samples ex-

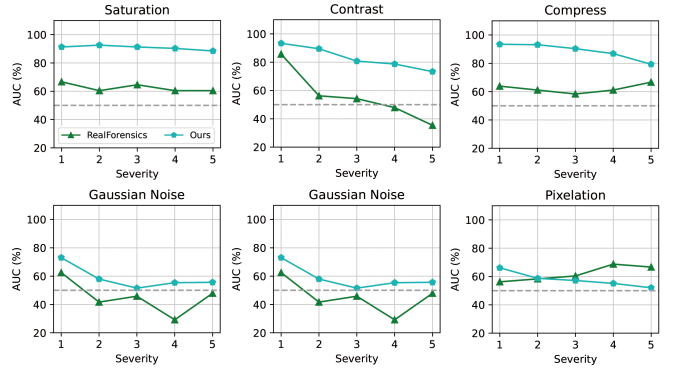


Figure 6: **Robustness against various unseen corruptions.** Average AUC scores across five intensity levels for various corruptions. For detailed analysis, please refer to the appendix.

posed to a set of perturbations. We investigate the performance of the detectors under six types of perturbation at five varying intensities. We use AUC score as evaluation metric, and the experimental results are presented in fig. 6. Evidently, our method outperforms the latest and the best DeepFake detectors RealForensics on most perturbation types.

Our approach effectively against saturation and contrast perturbations which performing linear transformations in the HLS space. For video compression, LipFD exhibits less corruption under varying levels of compression quality. Gaussian blur is applied by maintaining the size of the Gaussian kernel unchanged, while adjusting the standard deviation as the intensity. We find that both blurring and pixelation significantly degrade the performance of the detectors, likely due to the disruption of high-frequency information.

6 Ablation Studies

In this section, we present ablations to understand how our model works. Table 3 shows the overall situation of the experiment. Three significant components, Global feature encoder (E_G), Global-Region encoder (E_{GR}), and Region Awareness module, are ablated from the network separately, and their respective impact on the overall framework was reflected through changes in accuracy metric.

6.1 Global-Region encoder

Global-Region encoder takes cropped images and a vector encoded by the Global feature encoder as input, merging them into latent codes representing the correlation between regional parts and temporal sequence. The encoder E_{GR}

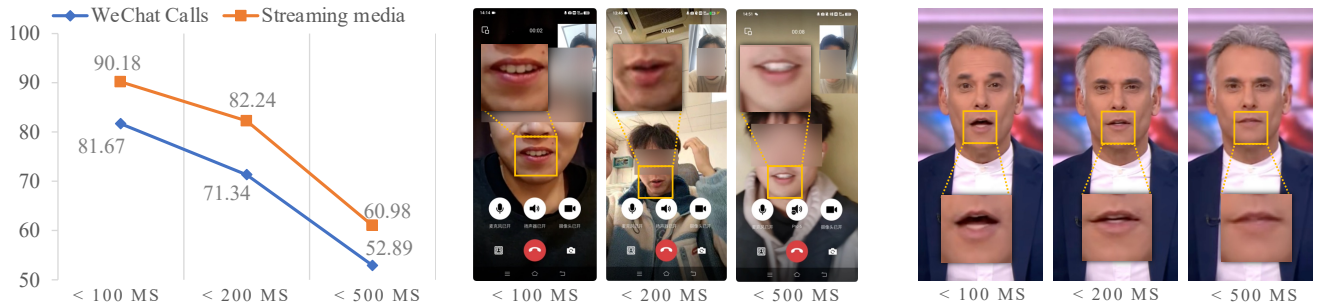


Figure 7: **Performance in real scenarios.** The x-axis represents network delay time, where a higher delay indicates a degradation in image transmission quality and clarity. Consequently, this degradation adversely impacts the audio-video synchronization in WeChat video calls.

Component	ACC \uparrow	AP \uparrow	FPR \downarrow	FNR \downarrow	AUC \uparrow
Global Encoder	95.07	91.81	0.02	0.07	95.09
Global-Region Encoder	72.52	64.38	0.01	0.53	72.50
Region Awareness	76.45	72.65	0.38	0.09	76.32
Full model (basic)	95.27	93.08	0.04	0.04	95.27

Table 3: **Overall ablation results.** Evaluation scores when components on the left column are stripped away individually.

plays a crucial role in the model. As shown in table 3, there is a significant drop in performance when E_{GR} is ablated.

In fig. 8 we visualized the gradients from the last layer of it using Grad-Cam. In the third line with the tag “lip”, the area near the lips has the deepest red color representing the highest gradient. The model focuses almost precisely on the shape of the entire lips. Meanwhile, in the above two lines, the encoder directs its attention to other features, specifically positional information, primarily on the bottom of the heads regardless of real or fake samples, for the reason that LipSync methods predominantly manipulate the bottom parts.

6.2 Region awareness module

The feature stack is assigned different weights by the modules based on their contributions to the discriminator. Subsequently, these features are fused to form the final feature vector. Higher weights indicate a dominant influence during the final judgment. We randomly selected some representative weights, which are shown in fig. 9. All weights are normalized according to the following formula:

$$\omega_i = \frac{w_i}{\omega_h + \omega_f + \omega_l}, \omega_i \in \{\omega_h, \omega_f, \omega_l\} \quad (8)$$

For the majority of forged video clips, the crops tagged as “lip” are assigned significantly higher weights than other re-

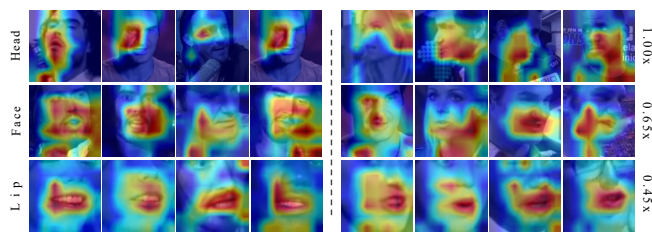


Figure 8: **Content sensitivity.** Left is real, right is fake. Visualization of the gradients from the last layer of the Global-Region encoder, which reflects the regions LipFD relies on.

	0.1158	0.1151	0.1088	0.1074	0.1040	0.1243	0.1333	0.1350	0.1245	0.1178	
Real											
Head	0.1158	0.1151	0.1088	0.1074	0.1040	0.1243	0.1333	0.1350	0.1245	0.1178	
Face	0.4830	0.4776	0.4784	0.4662	0.4597	0.4647	0.4677	0.4617	0.4342	0.4058	
Lip	0.4012	0.4074	0.4129	0.4264	0.4362	0.4110	0.3990	0.4033	0.4413	0.4764	
Fake											
Head	0.0595	0.0569	0.0479	0.0396	0.0394	0.0247	0.0268	0.0264	0.0234	0.0228	
Face	0.0871	0.0906	0.0904	0.0839	0.0862	0.1291	0.1436	0.1542	0.1871	0.2388	
Lip	0.8534	0.8525	0.8617	0.8766	0.8744	0.8462	0.8296	0.8194	0.7895	0.7385	

Figure 9: **The weights assigned by the module dynamically.** A higher numerical value indicates that the corresponding region of the image has a more significant impact on the final feature vector.

gions, indicating that these parts contain the most crucial contextual information for discrimination. On the contrary, our module leverages more information in larger-scale images (“face” and “head”) to form the latent code.

7 Performance in Real Scenarios

With the advancement of LipSync, certain forgery techniques have been employed for fraudulent purposes. To assess the practicality of our model in real-world scenarios, we conducted experiments across diverse network environments. Our model achieved up to **90.18%** accuracy in a network with latency below 100ms which is the common situation of daily life. Results are shown in fig. 7. For more details, please refer to our supplementary materials.

8 Conclusion

In this paper, we proposed LipFD, the first approach by exploiting temporal inconsistencies between audio and visual to detect lip forgery videos. LipFD demonstrates its efficacy in achieving high detection rates while exhibiting fabulous generalization to unseen data and robustness against various perturbations. We contribute AVLips, a high-quality audio-visual dataset for LipSync detection to the community, aiming to foster advancements in the domain of forged video detection. We hope our study encourages future research on lip-syncing DeepFake detection.

9 Technical Appendix

In the technical appendix, we present more details of our dataset AVLips, robustness evaluation, performance in real-scenario, discussion and future work.

References

- T. Afouras, J. S. Chung, A. Senior, O. Vinyals, and A. Zisserman. Deep audio-visual speech recognition. *arXiv:1809.02108*, 2018.
- Shruti Agarwal, Hany Farid, Ohad Fried, and Maneesh Agrawala. Detecting deep-fake videos from phoneme-viseme mismatches. In *2020 IEEE/CVF Conference on Computer Vision and Pattern Recognition Workshops (CVPRW)*, pages 2814–2822, 2020.
- Lucy Chai, David Bau, Ser-Nam Lim, and Phillip Isola. What makes fake images detectable? understanding properties that generalize. In *Computer Vision—ECCV 2020: 16th European Conference, Glasgow, UK, August 23–28, 2020, Proceedings, Part XXVI 16*, pages 103–120. Springer, 2020.
- Shen Chen, Taiping Yao, Yang Chen, Shouhong Ding, Jilin Li, and Rongrong Ji. Local relation learning for face forgery detection. In *Proceedings of the AAAI conference on artificial intelligence*, volume 35, pages 1081–1088, 2021.
- Yunjey Choi, Minje Choi, Munyoung Kim, Jung-Woo Ha, Sunghun Kim, and Jaegul Choo. Stargan: Unified generative adversarial networks for multi-domain image-to-image translation. In *Proceedings of the IEEE conference on computer vision and pattern recognition*, pages 8789–8797, 2018.
- Komal Chugh, Parul Gupta, Abhinav Dhall, and Ramanathan Subramanian. Not made for each other-audio-visual dissonance-based deepfake detection and localization. In *Proceedings of the 28th ACM international conference on multimedia*, pages 439–447, 2020.
- Davide Cozzolino, Alessandro Pianese, Matthias Nießner, and Luisa Verdoliva. Audio-visual person-of-interest deepfake detection. In *Proceedings of the IEEE/CVF Conference on Computer Vision and Pattern Recognition*, pages 943–952, 2023.
- Brian Dolhansky, Joanna Bitton, Ben Pfau, Jikuo Lu, Russ Howes, Menglin Wang, and Cristian Canton Ferrer. The deepfake detection challenge (dfdc) dataset. *arXiv preprint arXiv:2006.07397*, 2020.
- Shichao Dong, Jin Wang, Renhe Ji, Jiajun Liang, Haoqiang Fan, and Zheng Ge. Towards a robust deepfake detector: Common artifact deepfake detection model. *arXiv preprint arXiv:2210.14457*, 2022.
- Alexey Dosovitskiy, Lucas Beyer, Alexander Kolesnikov, Dirk Weissenborn, Xiaohua Zhai, Thomas Unterthiner, Mostafa Dehghani, Matthias Minderer, Georg Heigold, Sylvain Gelly, et al. An image is worth 16x16 words: Transformers for image recognition at scale. *arXiv preprint arXiv:2010.11929*, 2020.
- Alexandros Haliassos, Konstantinos Vougioukas, Stavros Petridis, and Maja Pantic. Lips don't lie: A generalisable and robust approach to face forgery detection. In *Proceedings of the IEEE/CVF conference on computer vision and pattern recognition*, pages 5039–5049, 2021.
- Alexandros Haliassos, Rodrigo Mira, Stavros Petridis, and Maja Pantic. Leveraging real talking faces via self-supervision for robust forgery detection. In *Proceedings of the IEEE/CVF Conference on Computer Vision and Pattern Recognition*, pages 14950–14962, 2022.
- Ammarah Hashmi, Sahibzada Adil Shahzad, Wasim Ahmad, Chia Wen Lin, Yu Tsao, and Hsin-Min Wang. Multimodal forgery detection using ensemble learning. In *2022 Asia-Pacific Signal and Information Processing Association Annual Summit and Conference (APSIPA ASC)*, pages 1524–1532. IEEE, 2022.
- Jonathan Ho, Ajay Jain, and Pieter Abbeel. Denoising diffusion probabilistic models. *Advances in neural information processing systems*, 33:6840–6851, 2020.
- Felix Juefei-Xu, Run Wang, Yihao Huang, Qing Guo, Lei Ma, and Yang Liu. Countering malicious deepfakes: Survey, battleground, and horizon. *International journal of computer vision*, 130(7):1678–1734, 2022.
- Tero Karras, Samuli Laine, and Timo Aila. A style-based generator architecture for generative adversarial networks. In *Proceedings of the IEEE/CVF conference on computer vision and pattern recognition*, pages 4401–4410, 2019.
- Hasam Khalid, Shahroz Tariq, Minha Kim, and Simon S Woo. Fakeavceleb: A novel audio-video multimodal deepfake dataset. *arXiv preprint arXiv:2108.05080*, 2021.
- Irene Kotsia, Ioan Buciu, and Ioannis Pitas. An analysis of facial expression recognition under partial facial image occlusion. *Image and Vision Computing*, 26(7):1052–1067, 2008.
- Asif Ali Laghari and Mureed Ali Laghari. Quality of experience assessment of calling services in social network. *ICT Express*, 7(2):158–161, 2021.
- Yongyuan Li, Xiuyuan Qin, Chao Liang, and Mingqiang Wei. Hdtr-net: A real-time high-definition teeth restoration network for arbitrary talking face generation methods. In *Chinese Conference on Pattern Recognition and Computer Vision (PRCV)*, pages 89–103. Springer, 2023.
- Ming Liu, Yukang Ding, Min Xia, Xiao Liu, Errui Ding, Wangmeng Zuo, and Shilei Wen. Stgan: A unified selective transfer network for arbitrary image attribute editing. In *Proceedings of the IEEE/CVF conference on computer vision and pattern recognition*, pages 3673–3682, 2019.
- Honggu Liu, Xiaodan Li, Wenbo Zhou, Yuefeng Chen, Yuan He, Hui Xue, Weiming Zhang, and Nenghai Yu. Spatial-phase shallow learning: rethinking face forgery detection in frequency domain. In *Proceedings of the IEEE/CVF conference on computer vision and pattern recognition*, pages 772–781, 2021.
- Kevin Lutz and Robert Bassett. Deepfake detection with inconsistent head poses: Reproducibility and analysis. *arXiv preprint arXiv:2108.12715*, 2021.
- Trisha Mittal, Uttaran Bhattacharya, Rohan Chandra, Aniket Bera, and Dinesh Manocha. Emotions don't lie: An audio-visual deepfake detection method using affective cues. In

- Proceedings of the 28th ACM international conference on multimedia*, pages 2823–2832, 2020.
- Sneha Muppalla, Shan Jia, and Siwei Lyu. Integrating audio-visual features for multimodal deepfake detection. *arXiv preprint arXiv:2310.03827*, 2023.
- Utkarsh Ojha, Yuheng Li, and Yong Jae Lee. Towards universal fake image detectors that generalize across generative models. In *Proceedings of the IEEE/CVF Conference on Computer Vision and Pattern Recognition*, pages 24480–24489, 2023.
- KR Prajwal, Rudrabha Mukhopadhyay, Vinay P Namboodiri, and CV Jawahar. A lip sync expert is all you need for speech to lip generation in the wild. In *Proceedings of the 28th ACM international conference on multimedia*, pages 484–492, 2020.
- Alec Radford, Jong Wook Kim, Chris Hallacy, Aditya Ramesh, Gabriel Goh, Sandhini Agarwal, Girish Sastry, Amanda Askell, Pamela Mishkin, Jack Clark, et al. Learning transferable visual models from natural language supervision. In *International conference on machine learning*, pages 8748–8763. PMLR, 2021.
- Nanditha Rao, A Maleki, F Chen, Wenjun Chen, C Zhang, Navneet Kaur, and Anwar Haque. Analysis of the effect of qos on video conferencing qoe. In *2019 15th International Wireless Communications & Mobile Computing Conference (IWCMC)*, pages 1267–1272. IEEE, 2019.
- Andreas Rossler, Davide Cozzolino, Luisa Verdoliva, Christian Riess, Justus Thies, and Matthias Nießner. Faceforensics++: Learning to detect manipulated facial images. In *Proceedings of the IEEE/CVF international conference on computer vision*, pages 1–11, 2019.
- Kaede Shiohara and Toshihiko Yamasaki. Detecting deepfakes with self-blended images. In *Proceedings of the IEEE/CVF Conference on Computer Vision and Pattern Recognition*, pages 18720–18729, 2022.
- Chao Shuai, Jieming Zhong, Shuang Wu, Feng Lin, Zhibo Wang, Zhongjie Ba, Zhenguang Liu, Lorenzo Cavallaro, and Kui Ren. Locate and verify: A two-stream network for improved deepfake detection. In *Proceedings of the 31st ACM International Conference on Multimedia*, pages 7131–7142, 2023.
- Supasorn Suwajanakorn, Steven M Seitz, and Ira Kemelmacher-Shlizerman. Synthesizing obama: learning lip sync from audio. *ACM Transactions on Graphics (TOG)*, 36(4):1–13, 2017.
- Hind Taud and JF Mas. Multilayer perceptron (mlp). *Geomatic approaches for modeling land change scenarios*, pages 451–455, 2018.
- Jiadong Wang, Xinyuan Qian, Malu Zhang, Robby T Tan, and Haizhou Li. Seeing what you said: Talking face generation guided by a lip reading expert. In *Proceedings of the IEEE/CVF Conference on Computer Vision and Pattern Recognition*, pages 14653–14662, 2023.
- Deressa Wodajo and Solomon Atnafu. Deepfake video detection using convolutional vision transformer. *arXiv preprint arXiv:2102.11126*, 2021.
- Wenyuan Yang, Xiaoyu Zhou, Zhikai Chen, Bofei Guo, Zhongjie Ba, Zhihua Xia, Xiaochun Cao, and Kui Ren. Avoid-df: Audio-visual joint learning for detecting deepfake. *IEEE Transactions on Information Forensics and Security*, 18:2015–2029, 2023.
- Zhenhui Ye, Jinzheng He, Ziyue Jiang, Rongjie Huang, Jiawei Huang, Jinglin Liu, Yi Ren, Xiang Yin, Zejun Ma, and Zhou Zhao. Geneface++: Generalized and stable real-time audio-driven 3d talking face generation. *arXiv preprint arXiv:2305.00787*, 2023.
- Yiru Zhao, Wanfeng Ge, Wenxin Li, Run Wang, Lei Zhao, and Jiang Ming. Capturing the persistence of facial expression features for deepfake video detection. In *Information and Communications Security: 21st International Conference, ICICS 2019, Beijing, China, December 15–17, 2019, Revised Selected Papers 21*, pages 630–645. Springer, 2020.
- Hanqing Zhao, Wenbo Zhou, Dongdong Chen, Tianyi Wei, Weiming Zhang, and Nenghai Yu. Multi-attentional deepfake detection. In *Proceedings of the IEEE/CVF conference on computer vision and pattern recognition*, pages 2185–2194, 2021.
- Yang Zhou, Xintong Han, Eli Shechtman, Jose Echevarria, Evangelos Kalogerakis, and Dingzeyu Li. Makeltalk: speaker-aware talking-head animation. *ACM Transactions On Graphics (TOG)*, 39(6):1–15, 2020.

A AVLips Dataset

In this section, we will provide a detailed description of the features.

A.1 Features

Dynamic expansion. The raw dataset consists of video files in MP4 format and audio files in WAV format. The videos are manipulated using state-of-the-art LipSync generation methods to forge lip movements. The original dataset can be dynamically expanded up to 60 times its initial size using the provided preprocessing code. The expanded samples are represented in the format shown in fig. 10. The randomness algorithm ensures that each expansion generates unique data, ensuring data diversity and providing a convenient data processing approach for temporal detection methods.

Real-world simulation. Since our ultimate goal is to achieve real-time detection in the real world, we employed seven perturbation methods listed in table 1, introducing various levels of perturbations to the images, to generate a substantial amount of robust training data. In addition, we have collected real-world samples from the internet, encompassing different scenes and varying levels of clarity to further enhance the diversity and realism of the dataset.

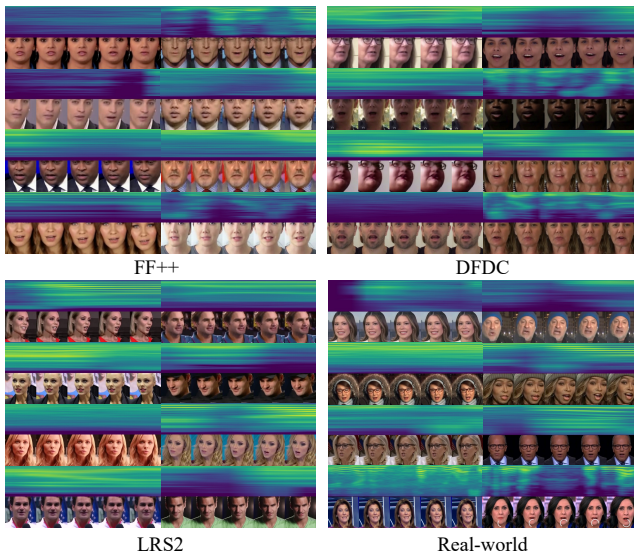


Figure 10: **Expanded data samples.** Each sample consists of T frames of video images and their corresponding audio spectra, serving as a temporal representation of the audio-visual context.

	Block Wise	Contrast	Saturation	Gaussian Blur	Gaussian Noise	Pixelation	Compression
Real							
Fake							
Ours	0.962	0.831	0.908	0.539	0.587	0.578	0.886
R.F.	0.625	0.563	0.624	0.504	0.454	0.621	0.622

Figure 11: **Perturbed samples and average results.** Real / Fake videos are corrupted using common perturbation methods at intensity level 3, followed by the extraction of video frames to obtain samples. Average AUC is the evaluation metric, indicating better robustness of detectors with higher values. R.F. stands for RealForensics detection.

B Robustness Evaluation

Due to the vulnerability of videos in the wild to varying degrees of corruptions, it is imperative for detectors not only to possess exceptional generalization capabilities but also to withstand common perturbations to accurately identifying fabricated videos. In this context, we investigate the performance of detectors under seven types of perturbations, each at five different intensity severity.

Experiment Setup. In our work, conducted without data augmentation, we train on the LRS2, FF++, and DFDC datasets and then expose test samples to previously unseen perturbations to examine the robustness of our detector. These perturbations encompass block-wise distortion, variations in contrast and saturation, blurring, Gaussian noise, pixelation, and video compression. As illustrated in table 1, the block-wise changes the number of blocks, with a higher count indicating more severe distortion. Contrast and saturation are

Type	Hyperparameter	Severity				
		1	2	3	4	5
Block-wise	Block number	16	32	48	64	80
Color Contrast	Pixel value	0.85	0.725	0.6	0.475	0.35
Color Saturation	YCbCr channel	0.4	0.3	0.2	0.1	0.0
Gaussian Blur	Gaussian kernel size	7	9	13	17	21
Gaussian Noise	Noise variance	0.001	0.002	0.005	0.01	0.05
Pixelation	Pixelation Level	2	3	4	5	6
Compression	Constant Rate Factor	30	32	35	38	40

Table 4: **Robustness experiment parameters.** Each perturbation method incorporates five distinct sets of hyperparameter values, exclusively altering the hyperparameters during the video preprocessing phase.

manipulated by altering the percentage of chrominance and luminance in video frames, where lower values correspond to greater corruptions. The blurring process entails adjustments to the size of the Gaussian kernel, and Gaussian white noise alters the variance of noise values. Video compression employs a constant rate factor to measure the ratio of video quality to size, with higher values denoting increased compression ratio.

Results Analysis. In the absence of any perturbations, the state-of-the-art detector, RealForensics Haliassos *et al.* [2022], exhibits performance that is second only to our method. However, Figure 1 shows a significant decline in the performance of RealForensics across the majority of perturbation types, whereas our method remains efficacious under most corruptions. Perturbations involving contrast and saturation engage the percentage of chrominance and luminance in the HLS space, where our detector maintains high AUC values, suggesting an effective retention of detection capabilities in diminished visual quality. However, the detector encounters a moderate decline in performance under conditions of blurring, Gaussian noise, and pixelation, though it still surpasses the RealForensics. This indicates the noise and reduced resolution impact the detector’s ability to accurately discern authenticity, potentially due to the refraction of high-frequency information. As for video compression, our approach exhibits remarkable resilience, achieving an average AUC of 0.886, which underscores the capacity of our detector to maintain high performance even when videos are subject to substantial compression, such as in real-world digital communications.

C Real-world Scenario

To better demonstrate the effectiveness of our proposed method in tackling the real threat of LipSync which is prevalent in the video call or financial frauds, we design and carry out extensive experiments to illustrate its practicability.

The quality of video calls and streaming clarity in the real world heavily relies on the quality of the network connection. Numerous applications employ algorithms such as ABR (Adaptive Bitrate) to dynamically adapt the audio and video bitrate and clarity, taking into account the user’s network conditions. However, this adaptive process may inadvertently introduce visual blurring and noise to the video. Additionally,

Latency	100ms		200ms	500ms
	CH	EN	EN	EN
WeChat video calls	72.53	81.67	71.34	52.89
Streaming media	74.41	90.18	82.24	60.98

Table 5: **Evaluation of Real-world scenarios.** Detection accuracy under various network delays and languages. CH stands for Chinese, and EN is in short for English.

network latency results in network jitter and packet loss and disrupts the synchronization between audio and video Rao *et al.* [2019]; Laghari and Laghari [2021], posing significant obstacles for accurate LipSync detection in real-world settings.

C.1 Setup

In order to simulate real-world network environments, we conducted experiments using an Android device with root access. Using the tc command, which is for network traffic control in Linux-based systems, we have the ability to manage network latency and packet loss.

We conducted a playback of the same video of a person speaking during WeChat video calls in three different network environments with varying levels of latency. Results indicate that as latency increases, the gap between audio and video timestamps widens.

C.2 Performance

Table 5 displays the accuracy of our model in two different real-world scenarios, aligning with the information presented in the line graph in the main text.

It is evident that the accuracy of our model in WeChat video calls is generally lower compared to streaming videos. This discrepancy can be attributed to our model’s strong reliance on the inconsistency between audio and video. As mentioned in our earlier analysis, as the latency increases, the audio gradually lags behind the video, creating a natural time difference that impedes our model’s performance. Conversely, in streaming videos, network latency primarily affects video bitrate and clarity, resulting in blurriness and noise reduction, while not significantly altering the synchronization between audio and video. Consequently, our model exhibits better overall performance in the task of streaming videos as opposed to video calls.

Apart from network condition, language also associates with performance. Videos with Chinese language under normal network condition result in much lower accuracy. Chinese and English have distinct pronunciation characteristics. The syllable and phoneme structures in Chinese differ from English. Moreover, Chinese has a flatter intonation pattern, while English exhibits more pitch variation and prosodic contours. These phonetic and prosodic differences can impact linguistic patterns, making the correspondence between lip movements and audio more complex in Chinese videos, thereby reducing the accuracy of LipSync detection, as LipFD relies on the consistency between lip movements and audio spectrum.

D Discussion and Future Work

Our method not only achieved high accuracy on the LRS2, FF++, and DFDC datasets but also demonstrated its effectiveness in real-world evaluations under normal network conditions. However, the performance of our model decreases considerably when faced with Non-English-speaking videos as mentioned in appendix C.2. So, it is crucial to incorporate multilingual training data to improve its accuracy and robustness in handling diverse linguistic contexts.

With the significant advancements in instant communication and large vision models (LVMs), generative models have made progress in achieving real-time cross-language forgery Ye *et al.* [2023]; Li *et al.* [2023]. The necessity of deploying a real-time LipSync detection system has come into the spotlight. Two research directions hold great promise:

- **Multilingual LipSync Detection.** Expanding LipSync detection to include multiple languages is an important area for future exploration. Investigating the challenges and differences in lip movements across various languages can contribute to developing more robust and accurate multilingual LipSync detection models.
- **Real-Time LipSync Detection.** Enhancing LipSync detection algorithms to operate in real-time scenarios is another significant research direction. Real-time detection is crucial for applications such as live streaming and video conferencing. Developing efficient and accurate algorithms that can process and analyze audio and video in real-time will be essential for these applications.